

# The mechanism of cellulose solubilization by urea studied by molecular simulation

Erik Wernersson · Björn Stenqvist · Mikael Lund

Received: 23 October 2014 / Accepted: 11 January 2015 / Published online: 20 January 2015  
© Springer Science+Business Media Dordrecht 2015

**Abstract** We used molecular dynamics simulation to model the effect of urea and thiourea on the solvent quality of aqueous solutions with respect to cellulose. A model system consisting of a periodically replicated cellulose molecule of effectively infinite degree of polymerization immersed in aqueous (thio-)urea solution was considered. Kirkwood-Buff theory, which relates the pair distribution functions to the concentration derivatives of the chemical potential, allowed the solubilization effect to be quantified in terms of the preferential binding of urea over water to the cellulose molecule. We found that urea is preferentially adsorbed on the hydrophobic faces of the anhydroglucose rings but has the same affinity as water to the hydroxyl groups. Thus, the simulations suggest that urea acts primarily by mitigating the effect of the hydrophobic portions of the cellulose molecule.

**Keywords** Solubilization · Urea · Thiourea · Molecular dynamics · Kirkwood-Buff theory

## Introduction

Cellulose is soluble in moderately concentrated (about 8–10 %w/w) sodium hydroxide solutions at

temperatures near freezing (Isogai and Atalla 1998; Heinze and Koschella 2005), but not to the extent that this ‘cold alkali’ solvent system is industrially significant. Cellulose dissolved in alkali is prone to form gels (Roy et al. 2003), which is an additional obstacle to industrial application. The performance can be improved, however, by introducing additives such as urea ( $\text{CO}(\text{NH}_2)_2$ ) or thiourea ( $\text{CS}(\text{NH}_2)_2$ ) (Cai and Zhang 2005). These additives do not remove the possibility of cellulose aggregation (Weng et al. 2004; Cai and Zhang 2006; Ruan et al. 2008; Zhang et al. 2010; Lue et al. 2011a, b), but can produce a solution that is kinetically stable over several days (Weng et al. 2004; Cai and Zhang 2006). The mechanism of action of urea and thiourea has attracted considerable attention in recent years and it has been suggested that (thio-)urea forms inclusion complexes with cellulose, thereby allowing them to dissolve on the molecular scale (Cai and Zhang 2005; Lue et al. 2007; Cai et al. 2007; Qin et al. 2013; Xiong et al. 2014). Surprisingly, differential scanning calorimetry has not revealed any strong NaOH–urea or urea–cellulose interactions in the alkali–urea solvent system (Egal et al. 2007; Isobe et al. 2013). Solid-state NMR does, however, suggest such interactions in solid NaOH–urea–cellulose mixtures obtained by freeze drying solutions (Song et al. 2014).

Urea is known as a general solubilizing agent for organic molecules (Wetlaufer et al. 1964; Pharr et al. 1989), and its mechanism of action is often described as an attenuation of the hydrophobic effect. As has

E. Wernersson (✉) · B. Stenqvist · M. Lund  
Division of Theoretical Chemistry, Department of  
Chemistry, Lund University, P.O. Box 124, 221 00 Lund,  
Sweden  
e-mail: erik.wernersson@fkem1.lu.se

been noted before (Bergensträhle-Wohlert et al. 2012; Isobe et al. 2013; Xiong et al. 2014), this is interesting in the context of the ‘Lindman hypothesis’ that hydrophobic interactions contribute significantly to the insolubility of cellulose (Lindman et al. 2010; Medronho et al. 2012; Glasser et al. 2012; Medronho and Lindman 2014). Cellulose is hydrophilic in many respects, but the faces of the pyranose rings can neither accept nor donate hydrogen bonds and act as hydrophobic patches. The two hydroxyl groups and the hydroxymethyl group of each anhydroglucose unit are all equatorially orientated, making the edges of the ribbon-like cellulose molecule hydrophilic. Thus, cellulose is an amphiphile, but unlike, e.g., surfactants the hydrophilic and hydrophobic parts are not readily identifiable ‘ends’ of the molecule but are in close proximity. The urea molecule, on the other hand, is highly polar and forms near-ideal solutions in water up to high concentrations, so its mechanism of action appears distinct from that of typical surfactants.

Urea has been known as a protein denaturant since the turn of the last century (Spiro 1900; Ramsden 1902). This is closely related to solubilization; improving the solvent quality with respect to hydrophobic amino-acid residues favors the swollen denatured state over the compact native fold. It is from studies on or motivated by protein denaturation that most of our knowledge of the, apparently general, urea solubilization mechanism originates and it is still an active area of research (Canchi and García 2013). In the early literature, the denaturing effect was mostly ascribed to direct interaction between urea and the chemically similar peptide bond. Such interactions do indeed play a role for the urea effect on proteins (Bolen and Rose 2008), but obviously cannot explain the effect on non-peptides. With the gradual understanding of the structure of liquid water and the hydrophobic effect (Kauzmann 1959), see Chandler (2005) for a modern review, came the notion that urea modifies hydrophobic solvation (Bruning and Holzer 1961; Nozaki and Tanford 1963). There has been some controversy about whether urea perturbs the global water structure in a way that makes it a better solvent for non-polar molecules (Frank and Franks 1968), or whether it facilitates the local solvation of hydrophobic groups by providing a greater variety of interaction opportunities (Nozaki and Tanford 1963). The latter explanation is favored in the recent literature, which

emphasizes direct interactions, see ref Canchi and García (2013) for a review.

Modern simulation studies point to a prominent role of dispersion forces for the effect of urea on proteins and simple model polymers (Hua et al. 2008; Zangi et al. 2009). In one of the few reported simulations of the interaction of cellulose with urea (Bergensträhle-Wohlert et al. 2012), urea enrichment at a cellulose fibril surface was explained by dispersion interactions. Urea is enriched at the hydrocarbon–water interface (Jones 1973), but slightly depleted at the air–water interface where there are no dispersion forces acting across the interface (Pegram and Record 2009). The purely enthalpic dispersion interaction, however, cannot be the sole explanation for the solubilizing effect of urea, as the transfer of simple hydrocarbons from neat water to urea solution is an endothermic process (Wetlaufer et al. 1964). Thus, dispersion forces and other enthalpic interactions between urea and the solute appear to be an enabling, rather than a driving, factor for the solubilization of hydrocarbons by urea. The very fact that urea is a larger molecule than water implies that a smaller number of degrees of freedom is restricted when urea replaces water in the solvation shell of a hydrophobic solute (Kuharski and Rossky 1984). A result that diverges from this general picture is a recent simulation study on cellulose in solution, where it is reported that urea mainly binds to the hydroxyl groups (Cai et al. 2012).

There are considerable chemical differences between proteins and carbohydrates. The main functional group of cellulose—non-phenolic hydroxyl—is present in only two of the twenty protein-forming amino acids and the fundamental motif of proteins—the peptide bond—has no counterpart in carbohydrates. Within proteins, there are significant differences in urea affinity between chemical motifs (Guinn et al. 2011), and the groups most abundant in carbohydrates, aliphatic carbon and hydroxyl oxygen, are reported to have only a weak affinity to urea. It is, therefore, unclear to what extent the conclusions about the mechanism of action of urea is transferable between proteins and carbohydrates. The modeling methodology developed for urea-peptide interaction has reached a considerable degree of sophistication (Weerashinghe and Smith 2003; Pierce et al. 2008; Horinek and Netz 2011; Canchi and García 2013), and should be generally applicable.

Here, we model the interaction between cellulose and urea by molecular dynamics (MD) simulations. Kirkwood-Buff (KB) theory (Kirkwood and Buff 1951), relates the molecular distribution functions to solution thermodynamic properties, and thus provides a rigorous theoretical framework for interpreting molecular simulations. The methodology for studying the effect of co-solvents on peptides within this framework provides both an adequately validated model for urea and a tractable route to quantify the effect of co-solvent (Weerasinghe and Smith 2003; Pierce et al. 2008; Horinek and Netz 2011). We combine this approach with a modern carbohydrate force field (Kirschner et al. 2008), to produce a detailed model of the cellulose–urea interactions that give rise to solubilization.

### Theoretical background

Within KB theory (Kirkwood and Buff 1951), the concentration derivatives of the chemical potentials in a multicomponent system can be expressed in terms of the correlations in composition fluctuations within a system. These are quantified as the KB integrals,

$$G_{ij} = \int (g_{ij}(\mathbf{r}) - 1) d\mathbf{r}, \quad (1)$$

where the integration is over the whole system. The pair distribution function,  $g_{ij}(\mathbf{r})$ , is a measure of the positional correlations in concentration of species  $i$  and  $j$ . Namely, the average concentration of species  $j$  at position  $\mathbf{r}$  relative to a particle of species  $i$  is  $c_j g_{ij}(\mathbf{r})$ , where  $c_j$  is the bulk molar concentration of  $j$ .  $g_{ij}(\mathbf{r})$  is dimensionless and  $G_{ij}$  have dimensions of volume or, equivalently, inverse concentration.

We follow the convention to denote the solvent (water), solute (cellulose), and co-solvent (urea or thiourea) by indexes 1, 2, and 3, respectively. The co-solvent effect on the solvent quality for a solute in infinite dilution can be expressed as

$$-\left(\frac{\partial \mu_2^0}{\partial \mu_3}\right)_{T,P} = c_3(G_{23} - G_{21}) = \Gamma_{23}, \quad (2)$$

where  $\mu_2^0$  is the solute standard chemical potential and  $\mu_3$  is the chemical potential of the co-solvent. The dimensionless quantity  $\Gamma_{23}$  is referred to as the preferential binding parameter, and is a measure of

relative propensity of the co-solvent to reside in the solute solvation shell compared to the solvent. The preferential binding parameter can be determined experimentally through osmometry (Pierce et al. 2008). The physical content of Eq. 2 is that species that adsorb on the solute surface to a greater extent than the solvent lowers the free energy cost of placing a solute molecule in the solution, i.e. improves the solvent quality. The co-solvent thus plays the same role as a surface active solute in the Gibbs adsorption isotherm,

$$-\left(\frac{\partial \gamma}{\partial \mu}\right)_{T,P} = \Gamma, \quad (3)$$

where  $\gamma$  is the surface tension,  $\mu$  is the solute chemical potential, and  $\Gamma$  is the solute surface excess per unit area. Solutes that preferentially adsorb at the water surface decreases the surface tension, the free energy cost of creating a unit area of surface. Comparison between Eqs. 2 and 3 shows that co-solvent has a closely analogous effect on the free energy cost of inserting the primary solute into the aqueous environment, see Shimizu and Matubayashi (2014) for an up-to-date discussion of surface tension in the framework of KB theory. Co-solvents can therefore be thought of as surfactants with respect to the solute-water interface. This surfactant action may or may not be correlated with ‘classical’ surfactant action at the air–water interface, depending on the properties of the solute.

The formalism for computing solubility from KB theory has been worked out in ref. Smith and Mazo (2008), and gives

$$\left(\frac{\partial \ln S_2}{\partial c_3}\right)_{T,P,\mu_2} = (G_{23} - G_{21})a_{33} \quad (4)$$

where  $S_2$  is the solubility, expressed as molar concentration of solute at saturation. This expression follows directly from eq 2 in the limit of infinite dilution, but is generally valid when the KB integrals pertain to a saturated solution. The activity derivative

$$a_{33} = \left(\frac{\partial \ln a_3}{\partial \ln c_3}\right)_{T,P}, \quad (5)$$

where  $a_3$  is the molar activity of the co-solvent, expresses the deviation of the co-solvent water solution from ideality. For not too high concentrations

of either solute or co-solvent, the KB integrals can be approximated by their infinite-dilution values, independent of concentration, and  $a_{33} \approx 1$ . Then, Eq. 4 can be integrated to give an expression analogous to the Sechenov equation (Gamsjäger et al. 2010)

$$\ln S_2/S_2^0 \approx (G_{23} - G_{21}) c_3, \quad (6)$$

where  $S_2^0$  is the solubility in neat solvent. These considerations show that  $G_{23}$  is a suitable quantity for evaluating co-solvent-induced changes in solvent quality from simulation data.

The preferential binding picture intrinsic to KB theory is in accord with the notion that (thio-)urea improves solubility by forming an inclusion complex with cellulose (Lue et al. 2007; Cai et al. 2007). KB theory shows that by the very fact that (thio-)urea improves solubility, there must be some region around the cellulose molecule in which (thio-)urea is enriched, effectively replacing water in the cellulose solvation shell. Note that since Eq. 4 relates the co-solvent binding to the logarithm of the solubility, the effect of co-solvent is multiplicative. Therefore, even a weak co-solvent binding can have a significant effect in a system where the solute is already somewhat soluble, such as cold alkali for cellulose. In addition, the KB integrals for the solute are on a per-molecule basis which means that a binding per monomer that would be insignificant if the monomer was a free compound can add up to be consequential even for polymers of modest length. Binding strengths that translate to interaction free energies of a fraction of the thermal energy per monomer would not necessarily be detected by calorimetric methods and, as noted in ref. Isobe et al. (2013), such consideration may explain the otherwise puzzling result that calorimetric studies seem to show no effect of urea (Egal et al. 2007; Isobe et al. 2013).

## Computational method

We considered a periodically replicated cellulose octamer, connected to its periodic images along the z-direction and thus mimicking an infinite chain, in a (thio-)urea–water solution. In addition to the cellulose molecule, the system contains 70, 140, or 280 urea molecules and 2,600 water molecules. This setup corresponds to cellulose in infinite dilution in urea

solutions of molal concentrations 1.5, 3, and 6 mol/kg, or 8, 15, and 26 % by weight. This concentration series roughly coincides with the range of reported concentrations of urea as an additive to the cold alkali solvent system. For thiourea, we only considered 1.5 mol/kg concentration, 10 % by weight, as this compound is significantly less soluble than urea. To investigate the role of the cellulose polarity, we carried out calculations for the hypothetical compound ‘non-polar cellulose’. These calculations were identical to those for cellulose in 1.5 mol/kg urea at 300 and 260 K except that they did not contain any electrostatic interactions involving cellulose. The simulations were preceded by a 10 ns equilibration run and propagated for 400–500 ns. The time step was 2 fs. Long-range electrostatics were handled using the particle-mesh Ewald method and the cut-off for short-range interactions was 0.8 nm (Essmann et al. 1995). The temperature was kept at 260 or 300 K using the Bussi thermostat (Bussi et al. 2007) and the pressure was kept at 1 bar using a weak coupling barostat (Berendsen et al. 1984), independently applied in the xy- and z-directions. The simulations were performed using GROMACS version 4.6.3. (Hess et al. 2008).

In all simulations, we used the GLYCAM06 force field for the cellulose molecule and the TIP4P/2005 model for water (Kirschner et al. 2008; Abascal and Vega 2005). For urea, the Lennard-Jones and bonded parameters were taken from GLYCAM06j. The partial charges and the N–C–N angle potential was taken from ref. Weerasinghe and Smith (2003), which has been shown to give a good representation of both bulk urea solution and urea-peptide interactions in calculations similar to those presented here (Horinek and Netz 2011). The Lennard-Jones parameters from the original paper are not suitable for combination with GLYCAM06 as different combination rules are used. Our slightly modified parameter combination was tested by computing the activity derivative for 3 mol/kg urea from a 50 ns simulation after a 1 ns equilibration of a system containing 216 urea and 4,000 water molecules. The resulting value  $a_{33} = 1.00 \pm 0.07$  agrees with the experimentally derived values reported in ref. Weerasinghe and Smith (2003), which are close to unity over the whole concentration range.

We adapted the urea force field for thiourea based on electronic structure calculations on urea and

thiourea. The geometries were optimized on the Hartree–Fock level with the ano-s-vdzp basis set (Almlöf and Taylor 1991), starting from the urea geometry. The resulting geometry was similar to the ones reported in ref. Puzzarini (2012). Partial charges, as determined by electrostatic potential fitting (ESPF), were computed from a single point calculation at the MP2 level with the ano-l-vtzip basis set on the optimized geometry. In these calculations, a polarizable continuum model was used to represent the solvent. All quantum mechanical calculations were performed using the Molcas software (Karlström et al. 2003). The Lennard-Jones parameters for thiourea sulfur were taken as sulfane sulfur from GLYCAM06. The C–S bond length was taken as 0.168 nm based on the optimized geometry. Rather than using the ESPF charges directly, we preserved the empirically optimized charges of the urea model for nitrogen and hydrogen. The thiourea sulfur partial charge was obtained by scaling the model urea oxygen partial charge by the ratio of the S and O ESPF charges from the thiourea and urea electronic structure calculations, resulting in an S partial charge of  $-0.467 e_0$ . The carbon partial charge was changed to 0.713 to maintain electroneutrality of the molecule. Otherwise, the thiourea model was identical to the urea model. While this parametrization procedure is unlikely to yield a globally optimal thiourea model, it does allow meaningful comparison to the urea model.

Evaluation of KB integrals require special considerations when using distribution functions from simulations with a constant number of particles. The pair distribution function in Eq. 1 must be evaluated in the grand canonical ensemble, where the system is free to exchange particles with its surroundings. The simulation box must be formally subdivided into ‘system’ and ‘surroundings’ at the analysis stage. The ‘system’ part will provide an adequate approximation to an open system if the ‘surroundings’ part is sufficiently large. We calculated the cellulose–urea and cellulose–water KB integrals from the excess coordination numbers  $\Delta N_{2j} = c_j G_{2j}$ , which give the excess number of particles of species  $j$  in the ‘system’ containing the cellulose molecule compared to the same volume of bulk solution. We take the ‘system’ to be a cylindrical region with radius  $R$  aligned along the cellulose molecule and centered on its center of geometry.  $N_{2j}^c(R)$  is the number of  $j$  molecules in the ‘system’ as a function of  $R$ . The function

$$\Delta N_{2j}(R) = N_{2j}^c(R) - V^c(R)c_j(R), \quad (7)$$

is an estimator of  $\Delta N_{2j}$  that becomes exact as the system size and  $R$  both go to infinity.  $c_j(R)$  is the average concentration of  $j$  in the ‘surroundings’,

$$c_j(R) = \frac{N_j - N_{2j}^c(R)}{V - V^c(R)}, \quad (8)$$

where  $N_j$  is the total number of particles of species  $j$  and  $V$ ,  $V^c(R)$  are the system and cylinder volume, respectively. We estimate  $G_{2j}$  as  $\frac{N_{2j}(R)}{c_j(R)}$  for  $R = 1$  nm. The preferential binding parameter can be evaluated from

$$\Gamma_{23}(R) = N_{23}^c(R) - N_{21}^c(R) \frac{N_3 - N_{23}^c(R)}{N_1 - N_{21}^c(R)}, \quad (9)$$

which is expedient because this expression does not require knowledge of the total volume.

## Results and discussion

The preferential binding parameter as well as the KB integrals are given in Fig. 1 as a function of concentration. In all cases  $\Gamma_{23}$  is positive, see Fig. 1a, consistent with the experimental fact that urea and thiourea tend to improve the solubility of cellulose. Note that this does not imply that the simulations predict that aqueous (thio-)urea solutions are cellulose solvents in themselves, but it does suggest that the mechanism of action of urea in the cold alkali system is not directly dependent on the presence of alkali. Rather, it suggests that urea improves the solvent quality and shifts the dissolution equilibrium by interacting favorably with cellulose in solution. The quantitative predictions about the effect of urea is testable for oligomeric cellulose with a degree of polymerization (DP) for which it is soluble without alkali. End effects would have to be addressed, but this is possible by repeating the calculation for the relevant DP or by repeating the solubility measurements for a few values of DP.

Thiourea shows a stronger preferential binding than urea, in agreement with the experimental fact that thiourea is a more powerful solubilizing agent (Lue et al. 2007). Urea shows a stronger preferential binding at the lower temperature than at the higher. This is consistent with recent solubility measurements (Isobe

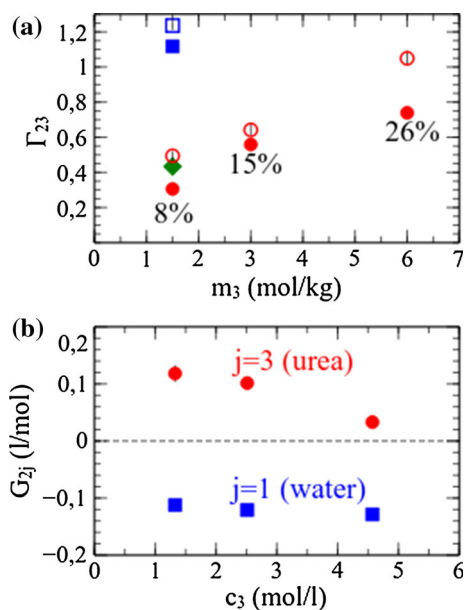


**Fig. 1** Top: preferential binding parameter  $\Gamma_{23}$  for cellulose in urea solution at temperatures 300 K (filled circle) and 260 K (open circle), for hypothetical non-polar cellulose in urea solution at 300 K (filled square) and 260 K (open square), and cellulose in thiourea solution at 300 K (filled diamond). The urea concentrations in mass percent is indicated; the point for thiourea corresponds to 10 % solution. Bottom: KB integrals corresponding to cellulose–urea ( $G_{23}$ , filled circle) and cellulose–water ( $G_{21}$ , filled square) for cellulose in urea solution at 300 K. The concentration in the lower panel is in molar units to be compatible with the KB integrals. In both panels, the quantities pertaining to cellulose are expressed per anhydroglycan unit. The size of the symbols is chosen to indicate the statistical error, as estimated by block averages, also visible as vertical lines in the open symbols

et al. 2013), where the relative increase in cellulose solubility in aqueous lithium hydroxide with compared to without urea was found to be slightly larger at lower temperature. This temperature dependence is in contrast to that for simple hydrocarbons, for which the solubilizing ability of urea improves with increasing, rather than decreasing, temperature (Wetlaufer et al. 1964). The concentration dependence appears to be affected by temperature as well, with the data for 300 K showing a more pronounced leveling-off at higher concentration. More data would be required to quantify this tendency, however. The binding of urea to ‘non-polar cellulose’ shows a weaker temperature dependence, especially in relative terms, which suggests that the binding has a weaker enthalpic driving force despite being stronger than for normal cellulose. The

considerable strength of urea binding to ‘non-polar cellulose’ reflects that the whole molecular surface of this hypothetical compound is hydrophobic. It thus appears that there are significant differences in the mechanism of urea solubilization of cellulose compared to simple hydrocarbons.

The KB integrals, in Fig. 1b, can be thought of as measures of the relative enrichment of one species in the vicinity of another. The cellulose–(thio-)urea KB integrals are positive, at least for the concentrations shown here, while the cellulose–water KB integrals are negative and nearly independent of concentration. A negative value of a KB integral between two species indicates that they displace each other due to excluded volume. The fact that water is the major component of the solution virtually guarantees that the cellulose–water KB integral is negative; even if there is strong affinity between the solute and water there is no room for the large excess of water molecules around the cellulose molecule that would be needed to offset its excluded volume. This does not apply to the co-solvent; the displaced number of molecules is considerably smaller due to the lower concentration and adsorption of urea on the cellulose molecule can be the dominant contribution. The decrease of  $G_{23}$  with concentration does, however, imply the onset of saturation of the urea binding. This is also reflected in the sub-linear increase of  $\Gamma_{23}$  with concentration.

The radial distribution functions involving cellulose  $g_{2j}(r)$ , i.e. the spherical averages of the pair distribution functions  $g_{2j}(\mathbf{r})$ , are shown in Fig. 2 for a selection of pairs of atomic species  $i$  and  $j$ . Note the choice of atoms for computing  $g_{2j}(r)$  does not influence the KB integrals, but different choices give different information about the local solvation structure. Furthermore the atom-centered  $g_{2j}(r)$  is impractical for calculating the KB integral due to long-range features from remote parts of the cellulose molecule. The structure factor that would be measured in a scattering experiment is proportional to a linear combination of the Fourier transform of the (atomic-nucleus centered) radial distribution functions. Figure 2 pertains to 1.5 mol/kg urea at room temperature. The difference between thiourea and urea and urea at different temperatures will be discussed below.

The three hydroxylic oxygen atoms, O2, O3, and O6, are well-solvated by both urea and water, as indicated by the sharp peaks in the radial distribution

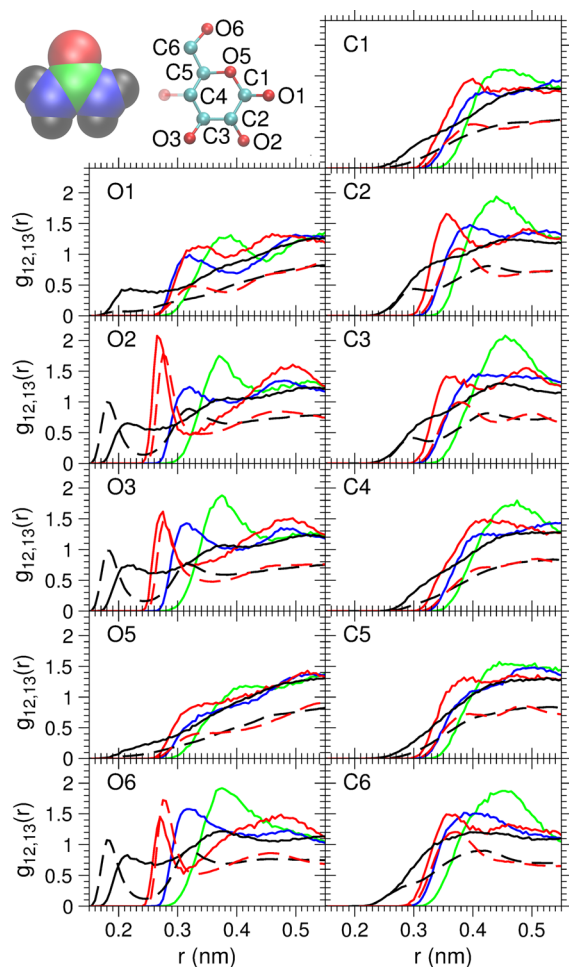


**Fig. 2** Cellulose–urea radial distribution functions (full curves) with respect to urea oxygen (red), carbon (green), nitrogen (blue) and hydrogen (black) and the corresponding cellulose–water radial distribution functions (dashed lines). The urea concentration is 1.5 mol/kg and the temperature is 300 K. (Color figure online)

functions pertaining to water and urea oxygen at a distance of 0.27 nm, corresponding to atomic contact and also roughly coinciding with the O–O distance in liquid water. This solvation does not contribute strongly to the preferential binding parameter, however, as it is almost equally strong for urea and water.

The two acetalic oxygen atoms, the glycoside linkage O1 and ring oxygen O5, are poorly solvated by water, but slightly better by urea. Thus, these are preferentially solvated in a way that contributes to the solubilization of cellulose. This is reflected in both urea oxygen and hydrogen radial distribution functions, the latter of which indicates that urea has a

significantly greater tendency to form hydrogen bonds with these oxygen atoms, especially O1, than water does.

The carbon atoms in the pyranose ring appear somewhat better solvated than the acetalic oxygen atoms. For C2 and C3, there is a pronounced peak for oxygen at 0.35 nm that, presumably, reflects the solvation of their adjacent hydroxyl groups. Carbons C1, C4 and C5 are solvated similar to O1, O5, but show a greater affinity for both urea and water oxygen. Also, the first peaks at a slightly greater distance due to the inaccessibility of these atoms compared to the acetalic oxygen atoms. That less accessible carbon atoms are better solvated than oxygen atoms may appear surprising. The ring carbon atoms, however, have significant positive partial charges, between 0.23 and 0.38  $e_0$  in the force field used here, and constitute a positive patch. The acetalic oxygens have partial charges of  $-0.47 e_0$ , compared to between  $-0.69$  and  $-0.71 e_0$  for the hydroxylic oxygens. A possible explanation for the relative degree of solvation of the acetalic oxygens and the adjacent ring carbons is thus that the former, though having considerable negative polarization, are not polar enough to accept hydrogen bonds from water in competition with other water molecules, but are polar enough to significantly repel water molecules approaching oxygen-first. The positive carbon atoms, in contrast, attract water molecules in this configuration.

The urea carbon radial distribution function shows a broad peak between 0.37 and 0.45 nm, regardless of the choice of reference atom in cellulose. This is larger than the distance that corresponds to atomic contact and shows that the urea molecules are oriented with either the oxygen or one of the  $\text{NH}_2$  groups towards cellulose. This does not necessarily mean that there is a strong affinity between these groups and cellulose, it may also reflect a smaller loss of favorable interaction with the aqueous environment. The N–H bond in urea is less polar than the O–H bond in water, and therefore urea N–H–water O hydrogen bonds are weaker than water–water hydrogen bonds. Therefore, the cost of a ‘dangling’, non H-bonding, urea N–H is smaller than the cost of a dangling water O–H.

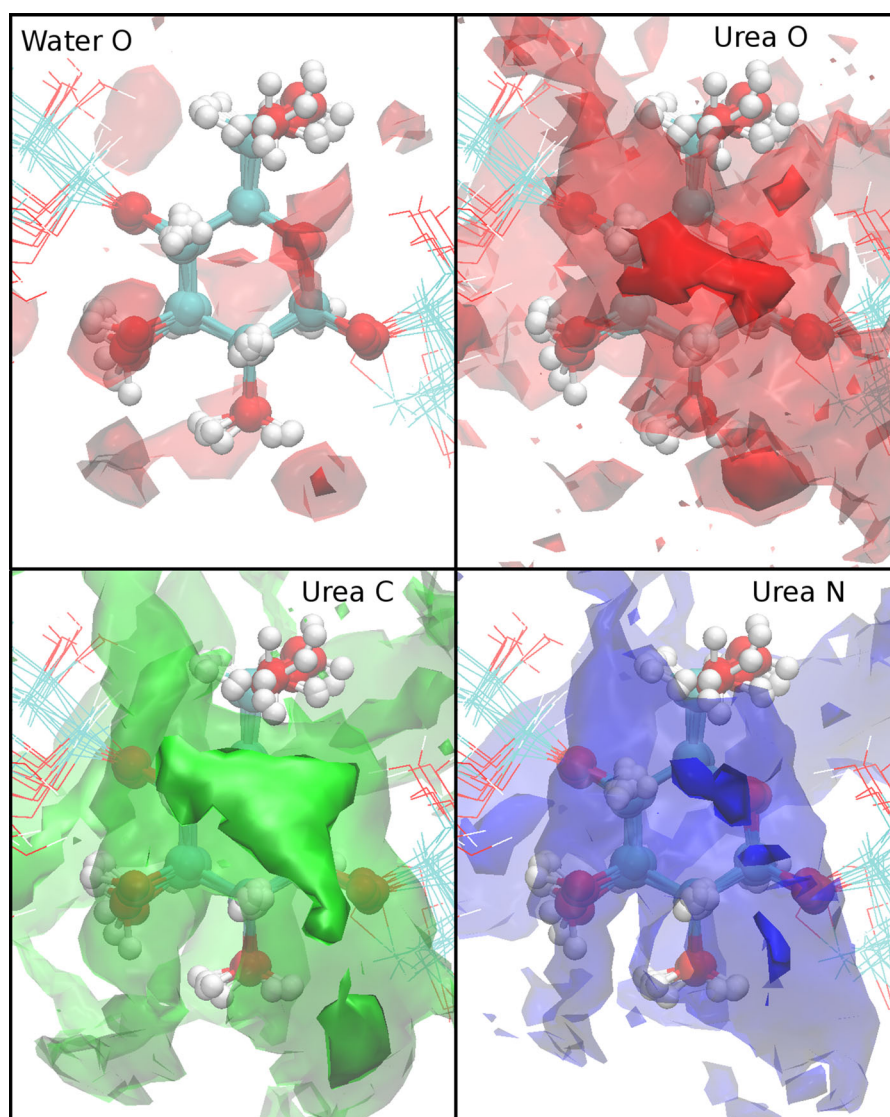
Isodensity surfaces of  $g_{2j}(\mathbf{r})$ , “density maps”, are shown for water oxygen and urea oxygen, carbon and nitrogen in Fig. 3. Water oxygen is preferentially located near the hydroxylic oxygen atoms of cellulose.

Urea oxygen occupies these sites as well, but can also be found above the ring face. It is this tendency to solvate the ring face that gives rise to the preferential solvation already discussed in connection with Fig. 2. The carbon density map shows less localization, which signifies that the carbon atoms in bound urea has more positional freedom than oxygen. Also, nitrogen can be seen to be enriched close to the glycoside oxygen, O1, which reflect urea's ability to donate hydrogen bonds to this atom.

The structural changes upon lowering the temperature and upon replacement of urea by thiourea and cellulose by 'non-polar cellulose' are shown in Fig. 4

in terms of the urea oxygen (thiourea sulfur) radial distribution functions. Note that the functions pertaining to atoms in cellulose with similar solvation structure have been averaged. Decreasing the temperature of the urea solution to 260 K results in an increased preferential binding to all groups, including the hydroxyl oxygens. The change is mostly in the adsorption of urea; the water-oxygen radial distribution functions change very little. Exchanging urea for thiourea at 300 K results in somewhat weaker binding to the hydroxyl groups, but a more strongly preferential binding to carbon and acetalic oxygen. Interestingly, the decrease in temperature has a similar effect

**Fig. 3** Isodensity surfaces of  $g_{2j}(\mathbf{r})$  for isovalues 3 (transparent surfaces) and 9 (opaque surfaces) for the atom types indicated. The cellulose position is taken as the center of geometry of an arbitrary anhydroglucose unit. The conformations of the cellulose molecules for ten randomly selected configurations are shown in order to give an impression of the conformational flexibility





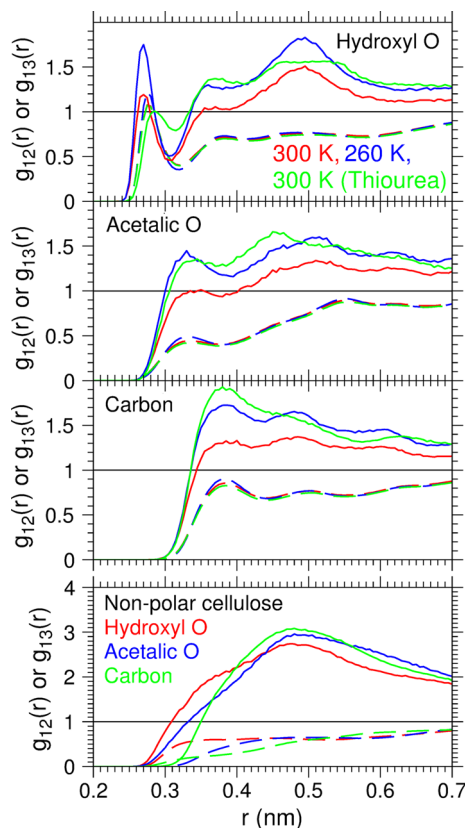


**Fig. 4** Upper three panels: full curves represent distribution functions for three cellulose groups with urea oxygen (thiourea sulfur) at 300 K (red), 260 K (blue), and thiourea sulfur at 300 K (green); Dashed curves represent the corresponding distributions with water oxygen. For the three hydroxylic oxygens (O2, O3, O6), the two acetalic oxygens (O1 and O5), and the carbon atoms have been averaged separately. In all cases, the (thio-)urea concentration is 1.5 mol/kg. Lower panel: Same, but for hypothetical non-polar cellulose in 1.5 mol/kg urea at 300 K. Here, the color coding indicates the cellulose atom categories: hydroxyl oxygen (red), acetalic oxygen (blue), and carbon (green). (Color figure online)

as the switch to thiourea on the latter binding. Although the fact that the change in binding strength is quantitatively similar is contingent on the choice of temperatures, the qualitative similarity is interesting. As expected, the hypothetical ‘non-polar cellulose’ is poorly solvated by water, with no peaks in the radial distribution function to indicate enrichment of water in the first solvation shell. The preferential solvation by urea is stronger than for the model actually intended to represent cellulose, and shows up as a broad, featureless peak with maximum at about 0.5 nm.

That the urea binding gets stronger with decreasing temperature implies that it is exothermic. As noted above, this is not the typical situation for organic molecules. It is consistent, however, with the notion of electrostatic interactions being an important part of the cellulose–urea interaction. This is further supported by the small temperature dependence for ‘non-polar cellulose’. Calorimetry data pertinent to the interactions between sugars and urea exist in the literature, but appears conflicting. The dissolution of cellobiose in pure water has been reported to become more endothermic with increasing concentration of urea but the dissolution in sodium hydroxide solution becomes more exothermic in the presence of urea (Zhao et al. 2013). Measurements of heat of dilution and mixing for urea and a range of sugars, including cellobiose, shows that that the urea–sugar interaction is exothermic (Barone 1990). As already noted above, direct comparison of cellulose solubility in the aqueous LiOH and LiOH/urea system does show a greater effect of urea at lower temperature (Isobe et al. 2013).

The carbon atoms of the pyranose ring of cellulose have a considerable positive partial charge and the acetalic oxygens are appreciably negative, making even the ring face more polar than an alkane of comparable size. As discussed above, the ring is still not sufficiently polar to compete with water for hydrogen bonds, see Fig. 2. The carbon and hydrogen atoms of urea have positive partial charges and it is easy to imagine that they can participate in the solvation of the ring face by aligning in a favorable configuration relative to the ring dipole. The simulation results indicate that this interaction is weak, but it might still be strong enough to explain the modest exothermicity of the urea–cellulose interaction implied by the inverse temperature dependence of the urea binding.

## Conclusions

Urea solubilizes cellulose by preferentially solvating the hydrophobic portions of the cellulose molecule, without interfering with the solvation of the hydrophilic parts. This is in line with the notion that urea mitigates the hydrophobic effect by reducing the entropy cost of accommodating the solute. In addition, the binding of urea to cellulose was found to be exothermic, in contrast to the interaction between urea

and simple hydrocarbons. From a technical, standpoint the results show that MD simulation is a practical way to evaluate the co-solvent effect on cellulose solubility on a semi-quantitative level, such as determining the rank order of efficiency of a series of potential co-solvents.

**Acknowledgments** For financial support the authors thanks Södra's Research Foundation; the Swedish Research Council; the Swedish Foundation for Strategic Research. For computational resources, LUNARC in Lund is greatly appreciated.

## References

- Abascal JLF, Vega C (2005) A general purpose model for the condensed phases of water: TIP4P/2005. *J Chem Phys* 123(234):505
- Almlöf J, Taylor PR (1991) Atomic natural orbital (ano) basis sets for quantum chemical calculations. *Adv Quantum Chem* 22:301–373
- Barone G (1990) Physical chemistry of aqueous solutions of oligosaccharides. *Thermochim Acta* 162:17–30
- Berendsen HJC, Postma JPM, van Gunsteren WF, DiNola A, Haak JR (1984) Molecular dynamics with coupling to an external bath. *J Chem Phys* 81:3684–3690
- Bergensträhle-Wohlert M, Berglund LA, Brady JW, Larsson PT, Westlund P, Wohlert J (2012) Concentration enrichment of urea at cellulose surfaces: results from molecular dynamics simulations and NMR spectroscopy. *Cellulose* 19:1–12
- Bolen DW, Rose GD (2008) Structure and energetics of the hydrogen-bonded backbone in protein folding. *Annu Rev Biochem* 77:339–362
- Bruning W, Holzer A (1961) The effect of urea on hydrophobic bonds: the critical micelle concentration of n-dodecyltrimethylammonium bromide in aqueous solutions of urea. *J Am Chem Soc* 83:4865–4866
- Bussi G, Donadio D, Parrinello M (2007) Canonical sampling through velocity rescaling. *J Chem Phys* 126(014):101
- Cai J, Zhang L (2005) Rapid dissolution of cellulose in LiOH/urea and NaOH/urea aqueous solutions. *Macromol Biosci* 5:539–548
- Cai J, Zhang L (2006) Unique gelation behavior of cellulose in NaOH/urea aqueous solution. *Biomacromolecules* 7:183–189
- Cai J, Zhang L, Chang C, Cheng G, Chen X, Chu B (2007) Hydrogen-bond-induced inclusion complex in aqueous cellulose/LiOH/urea solution at low temperature. *Chem-PhysChem* 8:1572–1579
- Cai L, Liu Y, Liang H (2012) Impact of hydrogen bonding on inclusion layer of urea to cellulose: study of molecular dynamics simulation. *Polymer* 53:1124–1130
- Canchi DR, García AE (2013) Cosolvent effects on protein stability. *Annu Rev Phys Chem* 64:273–293
- Chandler D (2005) Interfaces and the driving force of hydrophobic assembly. *Nature* 437:640–647
- Egal M, Budtova T, Navard P (2007) The dissolution of microcrystalline cellulose in sodium hydroxide-urea aqueous solutions. *Cellulose* 15:361–370
- Essmann U, Perera L, Berkowitz ML, Darden T, Lee H, Pedersen LG (1995) A smooth particle mesh Ewald method. *J Chem Phys* 103:8577–8592
- Frank HS, Franks F (1968) Structural approach to the solvent power of water for hydrocarbons; urea as a structure breaker. *J Chem Phys* 48:4746–4757
- Gamsjäger H, Lorimer JW, Salomon M, Shaw DG, Tomkins RPT (2010) The IUPAC-NIST solubility data series: a guide to preparation and use of compilations and evaluations (IUPAC technical report). *Pure Appl Chem* 82:1137–1159
- Glasser WG, Atalla RH, Blackwell J, Brown RM Jr, Burchard W, French AD, Klemm DO, Nishiyama Y (2012) About the structure of cellulose: debating the Lindman hypothesis. *Cellulose* 19:589–598
- Guinn EJ, Pegram LM, Capp MW, Pollock MN, Record MT Jr (2011) Quantifying why urea is a protein denaturant, whereas glycine betaine is a protein stabilizer. *Proc Natl Acad Sci USA* 108:16932–16937
- Heinze T, Koschella A (2005) Solvents applied in the field of cellulose chemistry: a mini review. *Polímeros* 15:84–90
- Hess B, Kutzner C, van der Spoel D, Lindahl E (2008) GRO-MACS 4: algorithms for highly efficient, load-balanced, and scalable molecular simulation. *J Chem Theory Comput* 4:435–447
- Horinek D, Netz RR (2011) Can simulations quantitatively predict peptide transfer free energies to urea solutions? Thermodynamic concepts and force field limitations. *J Phys Chem A* 115:6125–6136
- Hua L, Zhou R, Thirumalai D, Berne BJ (2008) Urea denaturation by stronger dispersion interactions with proteins than water implies a 2-stage unfolding. *Proc Natl Acad Sci USA* 105:16,928–16,933
- Isobe N, Noguchi K, Nishiyama Y, Kimura S, Wada M, Kuga S (2013) Role of urea in alkaline dissolution of cellulose. *Cellulose* 20:97–103
- Isogai A, Atalla RH (1998) Dissolution of cellulose in aqueous NaOH solutions. *Cellulose* 5:309–319
- Jones MN (1973) Interfacial tension studies at the aqueous urea-n-decane and aqueous urea + surfactant-n-decane interfaces. *J Colloid Interface Sci* 44:13–20
- Karlström G, Lindh R, Malmqvist PÅ, Roos BO, Ryde U, Veryazov V, Widmark PO, Cossi M, Schimmelpfennig B, Neogrady P (2003) Molcas: a program package for computational chemistry. *Comput Mater Sci* 28(2):222–239
- Kauzmann W (1959) Some factors in the interpretation of protein denaturation. *Adv Protein Chem* 14:1–63
- Kirkwood JG, Buff FP (1951) The statistical mechanical theory of solutions. I. *J Chem Phys* 19:774–777
- Kirschner KN, Yongye AB, Tschampel SM, Gonzalez-Outierino J, Daniels CR, Foley BL, Woods RJ (2008) Glycam06: a generalizable biomolecular force field. *carbohydrates. J Comp Chem* 29:622–655
- Kuharski RA, Rossky PJ (1984) Solvation of hydrophobic species in aqueous urea solution: a molecular dynamics study. *J Am Chem Soc* 106:5794–5800
- Lindman B, Karlström G, Stigsson L (2010) On the mechanism of dissolution of cellulose. *J Mol Liq* 156:76–81
- Lue A, Zhang L, Ruan D (2007) Inclusion complex formation of cellulose in NaOH/thiourea aqueous system at low temperature. *Macromol Chem Phys* 208:2359–2366

- Lue A, Liu Y, Zhang L, Potthas A (2011a) Investigation on metastable solution of cellulose dissolved in NaOH/urea aqueous system at low temperature. *J Phys Chem B* 115:12801–12808
- Lue A, Liu Y, Zhang L, Potthas A (2011b) Light scattering study on the dynamic behaviour of cellulose inclusion complex in LiOH/urea aqueous solution. *Polymer* 52:3857–3864
- Medronho B, Lindman B (2014) Competing forces during cellulose dissolution: from solvents to mechanisms. *Curr Opin Colloid In* 19:32–40
- Medronho B, Romano A, Miguel MG, Stigsson L, Lindman B (2012) Rationalizing cellulose (in)solubility: reviewing basic physicochemical aspects and role of hydrophobic interactions. *Cellulose* 19:581–587
- Nozaki Y, Tanford C (1963) The solubility of amino acids and related compounds in aqueous urea solutions. *J Biol Chem* 238:4074–4081
- Pegram LM, Record MT Jr (2009) Using surface tension data to predict differences in surface and bulk concentrations of nonelectrolytes in water. *J Phys Chem C* 113:2171–2174
- Pharr DY, Fu ZS, Smith TK, Hinze WL (1989) Solubilization of cyclodextrins for analytical applications. *Anal Chem* 61:275–279
- Pierce V, Kang M, Aburi M, Weerasinghe S, Smith PE (2008) Recent applications of Kirkwood-Buff theory to biological systems. *Cell Biochem Biophys* 50:1–22
- Puzzarini C (2012) Molecular structure of thiourea. *J Phy Chem A* 116(17):4381–4387
- Qin X, Lu A, Cai J, Zhang L (2013) Stability of inclusion complex formed by cellulose in NaOH/urea aqueous solution at low temperature. *Carbohydr Polym* 92:1315–1320
- Ramsden W (1902) Some new properties of urea. *J Physiol* 28:xxiii–xxvi
- Roy C, Budtova T, Navard P (2003) Rheological properties and gelation of aqueous cellulose/NaOH solutions. *Biomacromolecules* 4:259–264
- Ruan D, Lue A, Zhang L (2008) Gelation behaviors of cellulose solution dissolved in aqueous NaOH/thiourea at low temperature. *Polymer* 49:1027–1036
- Shimizu S, Matubayashi N (2014) Preferential solvation: dividing surface vs excess numbers. *J Phys Chem B* 118:3922–3930
- Smith PE, Mazo RM (2008) On the theory of solute solubility in mixed solvents. *J Phys Chem B* 112:7875–7884
- Song J, Ge H, Xu M, Chen Q, Zhang L (2014) Study on the interaction between urea and cellulose by combining solid-state  $^{13}\text{C}$  CP/MAS NMR and extended Hückel charges. *Cellulose* 21:4019–4027
- Spiro K (1900) Ueber die Beeinflussung der Eiweisscoagulation durch stickstoffhaltige Substanzen. *Z Physiol Chem* 30:182–199
- Weerasinghe S, Smith PE (2003) A Kirkwood-Buff derived force field for mixtures of urea and water. *J Phys Chem B* 107:3891–3898
- Weng L, Zhang L, Ruan D, Shi L, Xu J (2004) Thermal gelation of cellulose in a NaOH/thiourea aqueous solution. *Langmuir* 20:2086–2093
- Wetlaufer DB, Malik SK, Stoller L, Coffin RL (1964) Nonpolar group participation in the denaturation of proteins by urea and guanidinium salts. Model compound studies. *J Am Chem Soc* 86:508–514
- Xiong B, Zhao P, Hu K, Zhang L, Cheng G (2014) Dissolution of cellulose in aqueous NaOH/urea solution: role of urea. *Cellulose* 21:1183–1192
- Zangi R, Zhou R, Berne BJ (2009) Ureas action on hydrophobic interactions. *J Am Chem Soc* 131:1535–1541
- Zhang S, Li F, Yu J, Hsieh YL (2010) Dissolution behaviour and solubility of cellulose in NaOH complex solution. *Carbohydr Polym* 81:668–674
- Zhao X, Chen Y, Jiang X, Shang Y, Zhang L, Gong Q, Zhang H, Wang Z, Zhou X (2013) The thermodynamics study on the dissolution mechanism of cellobiose in NaOH/urea aqueous solution. *J Therm Anal Calorim* 111:891–896